

# SINTERIZAREA ÎN CÂMP DE MICROUNDĂ A ELECTROLIȚILOR DE GALAT DE LANTAN DOPAȚI CU Sr SI Mg (LSMG) MICROWAVE SINTERING OF Sr AND Mg-DOPED LANTHANUM GALLATE (LSGM) SOLID ELECTROLYTES

CRISTIAN ANDRONESCU<sup>1</sup>, VICTOR FRUTH<sup>1\*</sup>, ENIKÖ VOLCEANOV<sup>2</sup>, RAREȘ SCURTU<sup>1</sup>, CORNEL MUNTEANU<sup>1</sup>, MARIA ZAHARESCU<sup>1</sup>

<sup>1</sup>Institutul de Chimie Fizică „I.G. Murgulescu” al Academiei Române, Spl. Independenței 202, București 060021, România

<sup>2</sup>Institutul de Cercetări Metalurgice, Str. Mehadia 36, București 060543, România

*Sr<sup>2+</sup> and Mg<sup>2+</sup> simultaneously doped lanthanum gallate (LSGM) powders, prepared by a modified Pechini route using polyvinyl alcohol (PVA) as polymeric alcohol, were densified using an activated microwave technique at 2.45 GHz, to develop a dense stable electrolyte for application in intermediate temperatures solid oxide fuel cells (IT-SOFC). Thermal behaviour of precursors was investigated by means of differential thermal analysis combined with thermogravimetric analysis (DTA/TGA). The powders and sintered samples were characterized using scanning electron microscopy and energy dispersive analysis (SEM-EDAX), X-ray diffraction (XRD) and infrared spectroscopy (FT-IR). The thermal expansion coefficient (TEC) and ionic conductivity of the sintered samples were also evaluated. Fine, homogeneous and high density pellets of almost pure LSGM phase were obtained after sintering at 1400°C for a short period time in an activated microwave field. Using activated microwave field, due to the volumetric in situ heating, the sintering process is highly specific and instantaneous, leading to a faster kinetics compared to the conventional process (electric oven). With an optimized sintering schedule, a fine grained and dense microstructure of the samples were obtained.*

*Pulberea de galat de lantan dopat simultan cu Sr<sup>2+</sup> și Mg<sup>2+</sup>, preparată prin metoda Pechini modificată folosind alcoolul polivinilic (PVA) drept poliol, a fost densificată folosind tehnica activării în câmp de microunde la 2,45 GHz pentru a obține electroliți denși și stabili folosiți în alcătuirea pilelor de combustie cu electroliți solizi cu operare la temperaturi intermediare (IT-SOFC). Comportamentul termic al precursorilor a fost investigat prin analiză termică diferențială și termogravimetrie (DTA/TGA). Pulberile și probele sinterizate au fost caracterizate folosind microscopia electronică cu baleaj și analiza dispersiei energiei cu raze X (SEM-EDAX), difracție de raze X (XRD) și spectroscopie în infraroșu (FT-IR). Au fost de asemenea evaluate coeficientul de expansiune termică (TEC) și conductivitatea ionică a probelor sinterizate. Au fost obținute probe fine, omogene și cu densitate ridicată, constituite din faza LSGM aproape pură, după sinterizarea la 1400°C pentru perioade scurte de timp în câmp de microunde. Folosind activarea în câmp de microunde, datorită încălzirii volumetrică in situ, procesul de sinterizare este specific și instantaneu, determinând la o cinetică mai rapidă comparativ cu metoda convențională (cuptor electric). Folosind un program optimizat de sinterizare a fost obținută o microstructură fină și compactă a probelor.*

**Keywords:** solid electrolytes, LSGM, microwave technique, IT-SOFC.

## 1. Introduction

LSGM was first prepared by conventional ceramic method [1, 2] that was further reported in several other published papers [3-6]. However, the classical ceramic method presents several well known disadvantages, as follows: cannot provide controlled composition homogeneity, grain size uniformity and crystalline growth. The solid-state route results in hard agglomerates and coarser grains which inhibit sintering to obtain dense electrolyte materials. The ball milling of hard agglomerates may cause contamination from the milling and grinding medium.

Very often the resulting LSGM ceramic contains impurity phases. To remove impurity

phases, long reaction times (typically 10–40 h) and high temperatures are required. The high sintering temperature (~1500°C) required for the densification process of LSGM [4] often leads to the formation of a secondary phase such as LaSrGaO<sub>4</sub>, LaSrGa<sub>3</sub>O<sub>7</sub>, La<sub>4</sub>Ga<sub>2</sub>O<sub>9</sub> and MgO [7] due to its complex cations composition. This hinders the preparation of pure-phase LSGM at low thermal treatment temperatures. So, many researchers have turned to wet chemical synthesis methods such as sol–gel [8, 9], co-precipitation [10, 11], the amorphous citrate process [12], glycine-nitrate combustion method [13] Pechini method [14-16] or spray pyrolysis [17] to prepare the LSGM powders with relatively small grain sizes. Solution technique, provided homogeneity at all levels of processing,

\* Autor corespondent/Corresponding author,  
E-mail: vfruth@gmail.com

enabling synthesis of these oxides at lower temperature and consequently allowing higher densification.

On the other hand the synthesis method directly affects the density, microstructure and purity of the material. Microwaves are now being used in various technological and scientific fields in order to heat dielectric materials. Generally speaking, the microwave method needs a shorter reaction time and a lower temperature than the traditional ceramic method and the materials prepared by microwave irradiation have achieved beneficial results and applications. Many researchers have reported substitution of the microwave method for traditional solid-state synthesis [18-21]. Sol-gel synthesis and microwave sintering of  $\text{La}_{0.8}\text{Sr}_{0.2}\text{Ga}_{0.83}\text{Mg}_{0.17}\text{O}_{2.82}$  has been reported using gallium metal as a precursor and obtaining highly sintered mixed phases sample by microwave processing at  $1500^\circ\text{C}$  for 10 min [22].

The main advantage of using microwave heating is that the treatment time can be considerably reduced, which in many cases represents a reduction in the energy consumption, as well. Energy transfer from microwaves to reactants can be accomplished by direct irradiation or by a secondary heater. In microwave field, the heating behaviour of the reaction system is affected by many factors, such as the microwave irradiation power and the chemical composition, physical state, dielectric constant and dielectric loss of the reactants [23]. Microwave-induced chemical reactions can be used to solve problems associated with conventional surface heating because microwave heating is both internal and volumetric. The aim of this paper was to obtain dense LSMG ceramics by processing the corresponding powders obtained by the modified Pechini method and their sintering by a nonconventional technique using microwave activation.

## 2. Experimental

### 2.1. Powder synthesis and sample preparation

The powder synthesis was realized by the modified Pechini method. As it is well known this method supposes the previously formation of a gel. For any sol-gel synthesis, phase purity and sintered density of a product depends on the nature of the gel under identical charring conditions. To obtain a pure phase material with high sintered density under less extreme conditions, several synthetic trials need to be performed, which would involve optimization of several gelling parameters such as concentration of the precursor solution, concentration of citric acid, citric acid-polyol ratio and so on [14]. Strontium- and magnesia-doped lanthanum gallate corresponding to the formula :

$\text{La}_{1.8}\text{Sr}_{0.2}\text{Ga}_{1.83}\text{Mg}_{0.17}\text{O}_{2.81}$  was prepared through a modified Pechini route. All reagents used were of high purity (Merck):  $\text{La}(\text{NO}_3)_3 \cdot 6\text{H}_2\text{O}$ ,  $\text{Ga}(\text{NO}_3)_3 \cdot x\text{H}_2\text{O}$  (requires careful estimation prior to every synthetic process – by thermogravimetry in this work);  $\text{Mg}(\text{NO}_3)_2 \cdot 6\text{H}_2\text{O}$ ,  $\text{Sr}(\text{NO}_3)_2$ ,  $\text{C}_6\text{H}_8\text{O}_7$  and PVA  $[-(\text{CH}_2-\text{CH}(\text{OH})-n)]$   $n = 900$ . The ratio between LSMG precursors, citric acid and PVA was 1:2:0.002. Appropriate amounts of the salts were dissolved in distilled water separately to obtain solutions of 0.2M concentration that were then mixed and homogenized. To this solution, citric acid (0.6M) was added as a complexant. Polyvinyl alcohol (PVA) was added to enhance gelation (wt 5%). The resultant solution was slowly evaporated over a hot plate at  $70^\circ\text{C}/3$  hours and at  $80^\circ\text{C}/24$  hours in oven in order to form the gel. The so formed gel was heated in a heating mantle at  $400^\circ\text{C}$ , which resulted in a fine precursor powder and major release of the organics. The sintered samples were prepared from powder obtained by annealing at  $900^\circ\text{C}/1\text{h}$ , compacted into solid disks at 300 MPa and thermally treated in microwave field at  $1400^\circ\text{C}/30$  min. For comparison, similarly compacted solid disks were also sintered at  $1450^\circ\text{C}/6\text{h}$  in electrical oven. The densities of the sintered samples were evaluated using Archimedes's method.

The furnace used for this study was a 1.0 kW modified kitchen microwave oven. The modifications include a thermocouple type S (Pt-Rd) and a power controller (with both manual and automatic options) for temperature control. To sinter the specimens, two compacted samples were stacked, one on top and other centred on the floor of an insulation box, fabricated from low-density insulation board. Two SiC susceptors were placed inside the microwave furnace one at the bottom and the other on the top of the insulation box (Fig. 1). Once the box was positioned in the microwave filed, a power level was selected from the controller and the timer on the microwave set. During the run, the power was manually stepped and the temperature measured every minute. When the run was completed, the microwave door was opened. After approximately 40 minutes of cooling, the specimens were removed.

### 2.2. Characterization

Thermal analysis (DTA/TG) was performed with a Mettler Toledo 851° in air, with a heating rate  $10^\circ\text{C}/\text{min}$ .

Room temperature X-ray diffractometry (XRD) (ULTIMA IV, Rigaku) was performed on the synthesized powders and sintered samples with  $\text{CuK}_\alpha$  radiation. The same samples were also investigated by mean of FTIR spectrometry (Nicolet 6700).

The particle size and morphology of the as-prepared LSMG powders and sintered bodies were examined by scanning electron microscopy

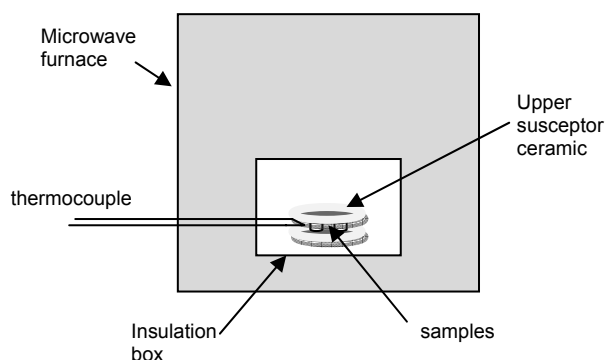


Fig. 1 - Schematic representation of the experiment setup  
 Reprezentarea schematică a modelului experimental de sinterizare în câmp de microunde.

(SEM) (FEI Quanta 3D FEG) equipped with an energy-dispersive spectrometer (EDX) (OXFORD INCA X-Sight, UK) system for elemental analysis.

The thermal expansion coefficient (TEC) was measured with a dilatometer (NETZSCH DIL 402C), from room temperature to 1000 - 1300°C. The dilatometer was calibrated by the NETZSCH Al<sub>2</sub>O<sub>3</sub> standard. A heating rate of 5C/min was adopted, using nitrogen as a purge gas.

Impedance spectroscopy measurements were performed with a Solartron 1260 FRA, in air, in the temperature range of 100 – 800 °C, and over the frequency range of 1 Hz – 3 MHz with amplitude of 100 mV. For a good contact with the electrodes the pellets were coated with silver paste on both sides and fired at 500 °C for 1 hour. The sample was placed in ProboStat sample holder from NorECs AS. Impedance data were corrected for the geometric factor of the sample (thickness/electrode area), the stray capacitance and inductance of the sample holder and the inductance of the measuring leads by using Zview fitting software.

### 3. Results and discussions

#### 3.1. Resin and resulted powders

In the case of sol-gel route, the complexation of the metal nitrate with the carboxylate ions forms sols and adding a polyol (polyvinyl alcohol - PVA) forms gel. The PVA helps in esterifying the carboxylic acid and subsequently ends up in forming a resin like product. The resin does not stick to the wall of the glass beaker in which the preparation was made.

The results of thermal analysis (TGA/DTA) of the LSGM samples prepared in this study are given in Fig. 2. The DTA curve of LSGM resin (Fig. 2a) showed exothermic peaks at 353°C, 394°C, 420°C, and 606°C. These events may be assigned to decompositions and pyrolysis of different organics resulted during heating. The first two exotherms may be associated with charring of the polymer, while the peak at 420°C was associated

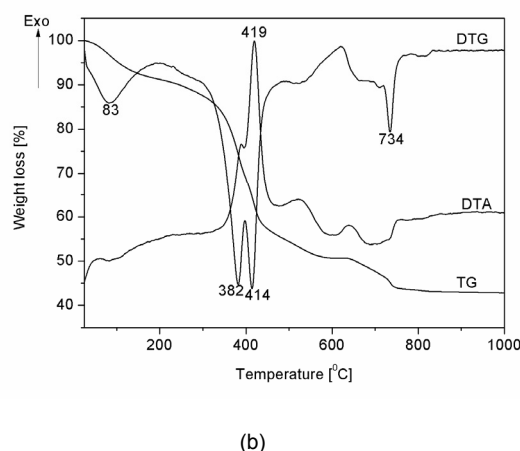
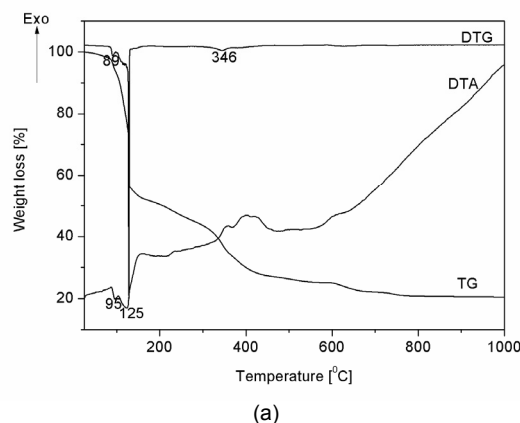


Fig. 2 - DTA/TG curves of LSGM resin (a) and powders obtained after combustion at 400°C (b) / Curbele termice DTA/TG ale rășinii (a) și pulberii obținute după combustia la 400°C (b).

with the pyrolysis of the organics. The last effect at 606°C resulted also from char burnout, in agreement with Tas *et al.* [24]. TG analysis showed that most of the weight loss occurred in the 100-450°C temperature range. (79.2 wt%). The thermal behaviour of the obtained powders after thermal treatment in the heating mantel (400°C) is presented in the Fig. 2b. The total weight loss carried-on progressively up to 1000°C, was 56.3%, inferring the idea that the combustion process was not finished after calcinations at 400°C, the organic fragments being not completely burn-out. The annealed powders at 900°C/1h have presented 1.5 wt% weight loss up to 1500°C (figure was not presented here). Change slopes on the Tg curve were noticed at 430°C, 740°C and 1020°C respectively. The endothermic events may be associated with solid state reactions occurring in the system.

The thermal events identified by DTA/TG analysis are in good agreement with FT-IR data. FT-IR spectroscopy plots of the LSGM samples depending on the thermal treatment temperatures are given in Fig. 3.

From the decrease in the intensity of the

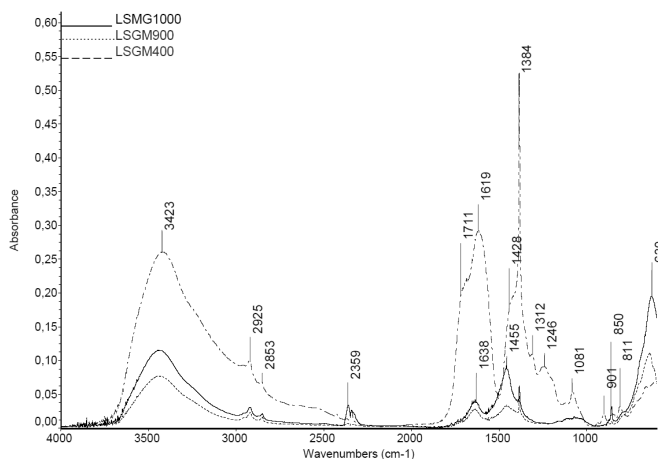
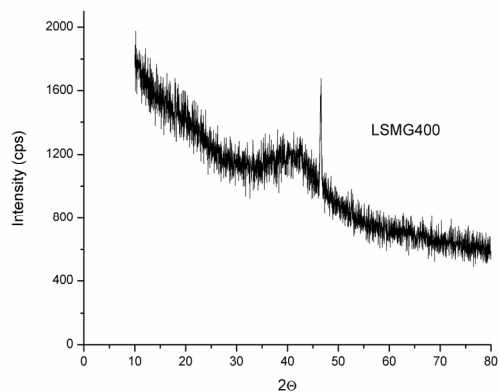


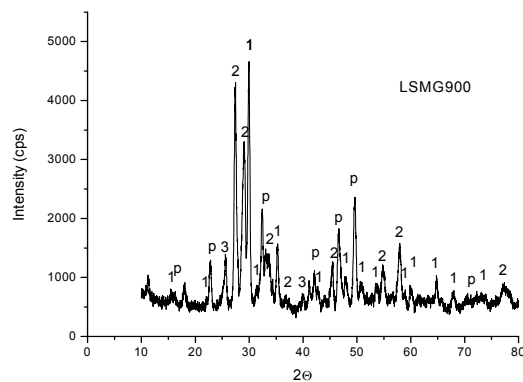
Fig. 3 - FTIR spectra of the intermediate products: calcinated resin at 400°C (full line) and annealed for 1 hour at 900°C (dotted line) or 1000°C (dashed line), respectively / *Spectrele FTIR ale produşilor intermediari: raşina calcinată la 400°C (linia plină) şi tratată termic 1 ora la 900°C (linia punctată) sau 1000°C (linia întreruptă).*

bands due to citrate/carboxylate groups and the lower intensity of the H<sub>2</sub>O stretching band (3500-3200 cm<sup>-1</sup>), one may conclude that the metal-carbonyl links begin to break after heating at 400°C (Fig. 3). The strong band at 1384 cm<sup>-1</sup> was attributed to the presence of nitrate anions and the absorption band at 1428 cm<sup>-1</sup> was due to the stretching modes of C=O functional groups. The bands at 1081 cm<sup>-1</sup>, 850 cm<sup>-1</sup> and 811 cm<sup>-1</sup> are assigned to the symmetric stretching and bending modes of carbonate ions. Samples that were annealed at 900°C basically show the CO<sub>3</sub><sup>2-</sup> and H<sub>2</sub>O vibrations in their IR spectra. After annealing at 1000°C, all IR bands that were attributed to anion vibrations disappeared in all samples. The bands which appear in the 700 - 500 cm<sup>-1</sup> range are assigned to M - O stretching vibrations in an octahedral geometry and one may noticed that the absorption intensities increased with the thermal treatment temperatures.

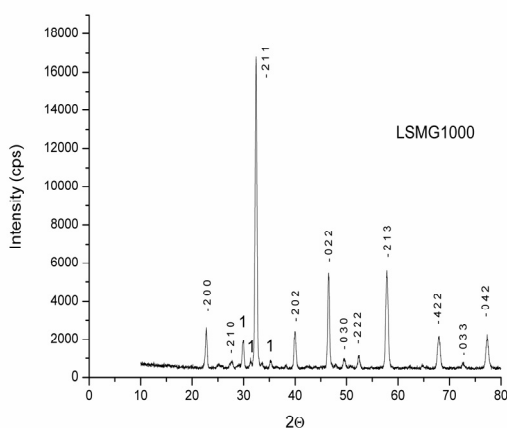
The evolution of the phases from the resin state to well-crystallized powders was investigated by XRD. The results are presented in Fig. 4.



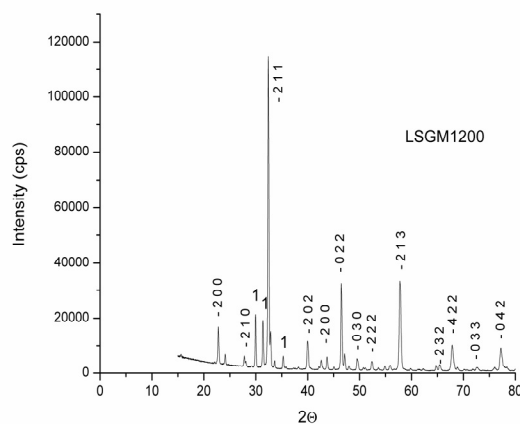
a



b



c



d

Fig. 4 - XRD patterns of samples after different annealing treatments: - 400 °C (a); 900°C/1h (b); 1000°C/1h (c) and 1200°C/1h (d); "p" – LSGM perovskite phase, "1" – SrLaGa<sub>3</sub>O<sub>7</sub> peaks, "2" - La<sub>4</sub>Ga<sub>2</sub>O<sub>9</sub> peaks, "3" – SrLaGaO<sub>4</sub> peaks. Indexed lines belong to the LSGM phase. / *Linii de difracţie XRD ale probelor, după diferite tratamente termice: - 400 °C (a); 900°C/1h (b); 1000°C/1h (c) si 1200°C/1h (d); "p" – LSGM faza perovskitică, "1" – SrLaGa<sub>3</sub>O<sub>7</sub> linii caracteristice, "2"- La<sub>4</sub>Ga<sub>2</sub>O<sub>9</sub> linii caracteristice, "3" – SrLaGaO<sub>4</sub> linii caracteristice. Linii indexate aparţin fazei LSGM.*

The XRD pattern of the resin thermally treated at 400°C, is presented in the Fig. 4a, showing that the resulted powder is mainly amorphous. The very small diffraction lines at  $2\theta = 46^\circ$  and  $61^\circ$  could be assigned to the presence of formed strontium carbonate (013 line), in good agreement with the FT-IR results.

The powder resulted after resins annealing at 400°C and consequently thermally treated at 900°C, for 1 h, presented the X-ray diffraction pattern shown in Fig. 4b. The diffraction lines are assigned to the LaSrGa<sub>3</sub>O<sub>7</sub> JCPDS [45-0637], and to a perovskite phase with the orthorhombic symmetry, with the following cells parameters:  $a = 5.521 \text{ \AA}$ ,  $b = 5.530 \text{ \AA}$  and  $c = 7.801 \text{ \AA}$ . Besides these phases the X-ray diffraction lines of the secondary phases La<sub>4</sub>Ga<sub>2</sub>O<sub>9</sub> [53-1108] and SrLa(GaO<sub>4</sub>) – JCPDS [80-1806] were identified.

The diffraction lines of the previous powder, supplementary thermally treated at 1000°C, are presented in the Fig. 4c. It could be noticed that LSGM perovskite phase with an orthorhombic symmetry and with the following cell parameters  $a = 5.534 \text{ \AA}$ ,  $b = 5.513 \text{ \AA}$ ,  $c = 7.818 \text{ \AA}$  is the dominate constituent. The presence of a secondary phase is still observed and it represents the LaSrGa<sub>3</sub>O<sub>7</sub> with a tetragonal symmetry with the following cells parameters  $a = b = 8.060 \text{ \AA}$ ,  $c = 5.335 \text{ \AA}$ .

However, if the powder obtained after the 400°C thermally treatment is annealed directly at 1200°C for 1 h, a well crystallized LSGM perovskite phase with orthorhombic symmetry and with the

following cell parameters:  $a = 5.536 \text{ \AA}$ ,  $b = 5.517 \text{ \AA}$  and  $c = 7.825 \text{ \AA}$  is obtained (Fig. 4d). Some secondary phases are also present. The supplementary diffraction lines were assigned mainly to LaSrGa<sub>3</sub>O<sub>7</sub> and SrLa(GaO<sub>4</sub>).

From the presented results it can be noticed that LSGM powder with perovskite structure is obtained already by the thermal treatment at 900°C/1h, but secondary phases are still present.

By a supplementary thermal treatment at 1000°C/1h the perovskite phase represents the main phase with a high degree of crystallinity. However, the secondary phases persist.

The thermal treatment at 1200°C/1h of the powder obtained by the resin combustion gives a similar result as mentioned above, namely well crystallized LSGM perovskite phase and low amount of secondary phases.

The morphology of the LSGM powders, as a function of thermal treatment temperature, was exhibited in the SEM images that are shown in Fig. 5. The initially amorphous resin began to crumble at temperatures of 400°C forming a mixture of big (tens microns) and small (microns) chunks (Fig. 5a-b). Cavities, in micrometric range, formed inside of the chunks after the combustion reactions by releasing the gaseous products can be noticed. Further calcinations at 900°C/1h have produced agglomeration and crystallization of small particles (Fig. 5c-d). After thermal treatment at 1000°C for 1 hour, it is evident that all the chunks were composed of small particles (100-200 nm) linked together in a three-dimensional network (5e-f).

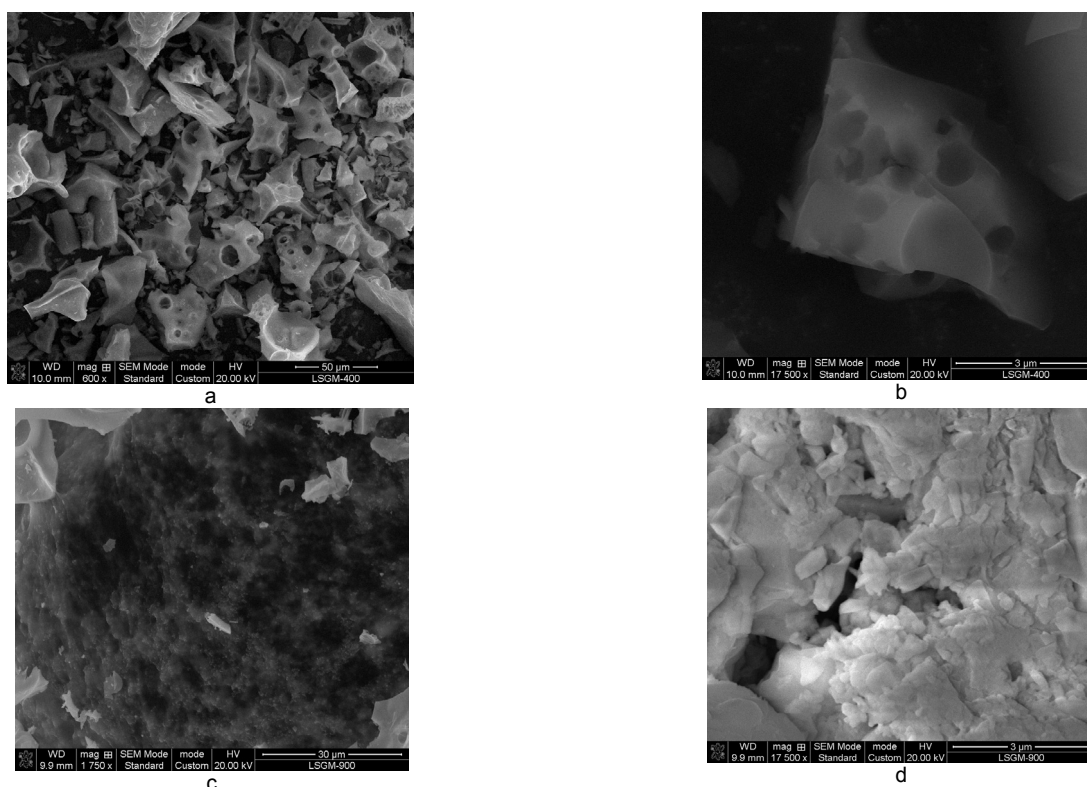


Fig. 5 - continues on next page/se continuă pe pagina următoare

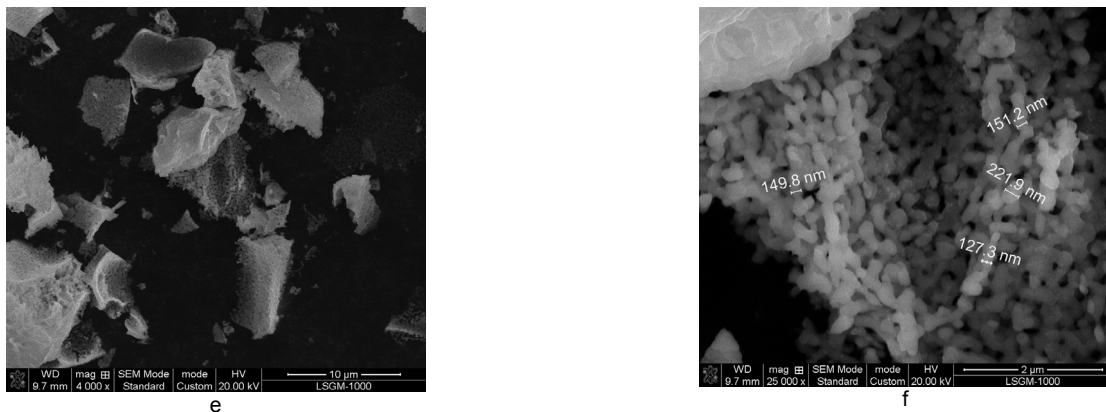


Fig. 5 - SEM images of LSGM powders calcined at different temperatures [(a-b) 400°C –after combustion, (c-d) 900°C/1h , and (e-f) 1000°C/1h]. *Imagini SEM ale pulberilor calcinate la diferite temperaturi [(a-b) 400°C – după combustie, (c-d) 900°C/1h , și (e-f) 1000°C/1h].*

In addition, EDX results proved that the powders after combustion (400°C) contain carbon (burned and remained organics) 30-34% and nitrogen 1.6-2%.

Based on the EDX data, the following compositions of the LSGM could be calculated:  $\text{La}_{0.96}\text{Sr}_{0.149}\text{GaMg}_{0.26}\text{O}_x$  and  $\text{La}_{0.98}\text{Sr}_{0.109}\text{GaMg}_{0.09}\text{O}_y$ . The differences in the mentioned compositions from the calculated one could be assigned to the formation of the secondary phases.

### 3.2. Sintered ceramics

The X-ray diffraction lines of the samples sintered in microwave field are presented in Fig. 6a. The indexed lines corresponds to the perovskite phase, while the low intensity lines (noted with \*) are assigned to a small amount of an unidentified secondary phase. LSGM phase has an orthorhombic symmetry confirmed by the splitting of the peaks located at 57.7°, 67.7° and 77.2°. Cell parameters were  $a = 7.806 \text{ \AA}$ ,  $b = 5.524 \text{ \AA}$  and  $c = 5.530 \text{ \AA}$ . This finding about the crystal structure of LSGM phase is consistent with the observation of Slater *et al.* [25] and Tas *et al.* [24]. Contrary, when the same sample was sintered in an electrical oven the crystal structure of LSGM was cubic with  $a = 3.909 \text{ \AA}$  and the amount of the secondary  $\text{SrLaGa}_3\text{O}_7$  phase was over 5% (fig. 6b).

The thermal treatment in microwave field at 1400°C/30 min of the powder thermally treated at 900°C/1h, enhanced the crystallinity of the LSGM perovskite phase but did not eliminate totally the presence of the secondary phase.

Mean relative density values of  $6.35 \text{ g/cm}^3$  (95%) and  $6.15 \text{ g/cm}^3$  (92%), were obtained for the microwave sintered samples and for the classically sintered samples, respectively, in accordance with SEM observations. The theoretical density was established as  $6.68 \text{ g/cm}^3$ .

The morphology of the sintered ceramics in the microwave field is presented in Fig. 7a-b, as compared to the similar samples sintered by conventional method (Fig. 7c-d). One may notice

highly-densified ceramics in the case of microwave sintering, while by conventional sintering well-crystallized ceramics, but with a certain amount of intergranular porosity were obtained.

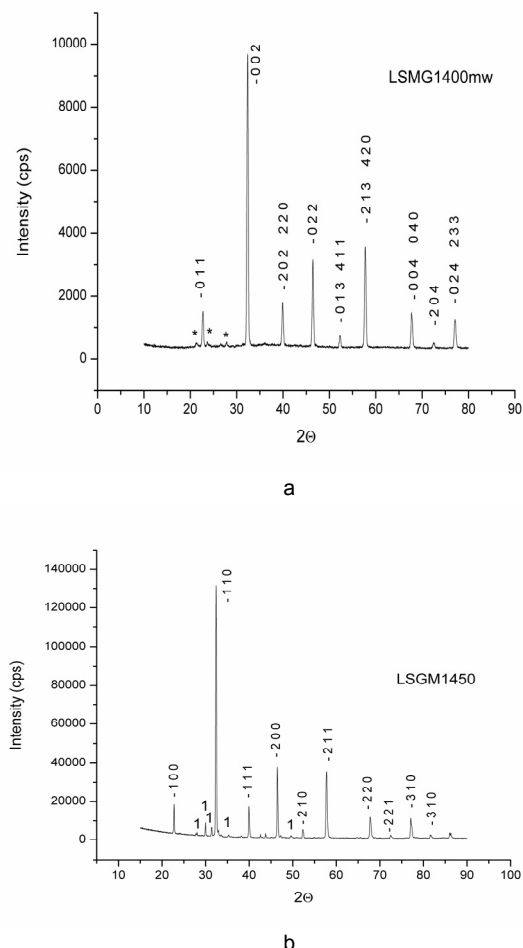


Fig. 6 - XRD patterns of LSGM phase sintered by activate microwave irradiation - at 1400°C/30 minutes (a) and in a classical electrical oven - at 1450°C/6 hours (b); "1" –  $\text{SrLaGa}_3\text{O}_7$  peaks, "\*" unidentified phase., mw – microwave / *Spectrele de difracție XRD ale fazei LSGM obținute prin sinterizare în câmp de microunde -1400°C/30 minute (a) și în cuptorul electric clasic - 1450°C/6 ore (b); "1" –  $\text{SrLaGa}_3\text{O}_7$  linii caracteristice, "\*" neidentificat, mw -microunde.*

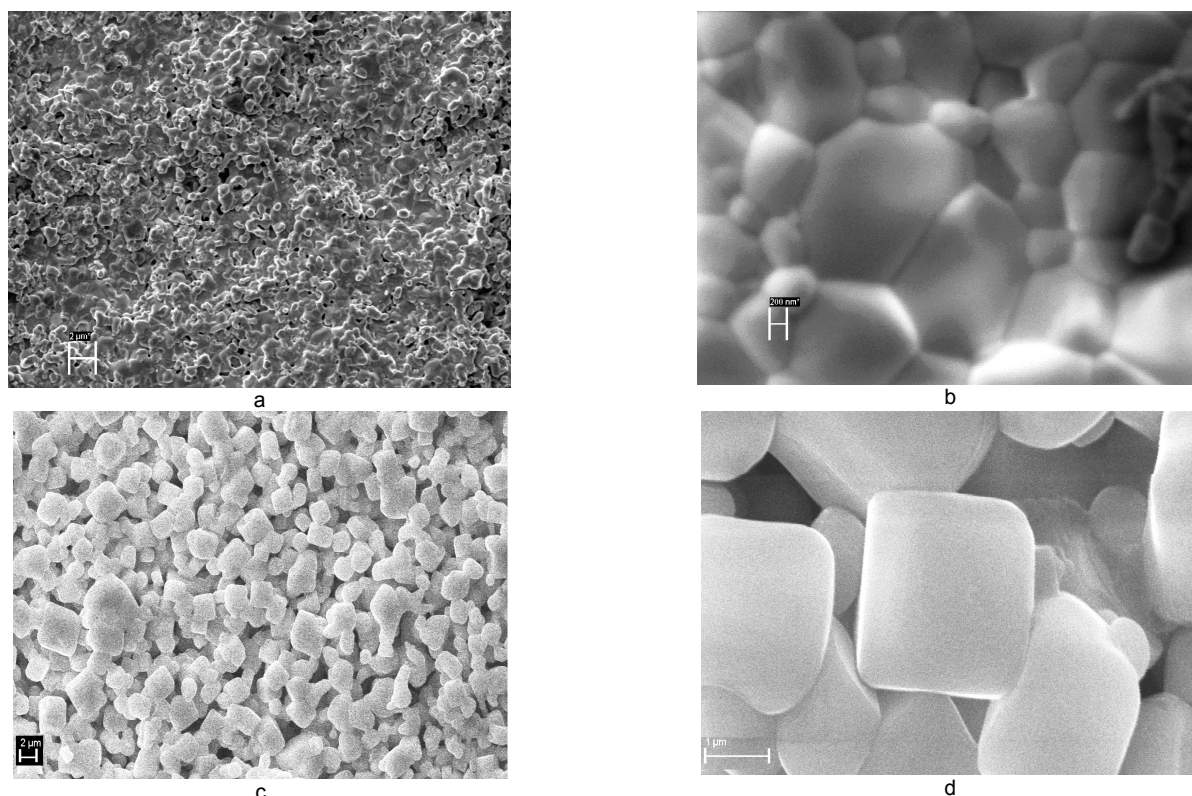


Fig. 7 - SEM images of LSGM samples sintered in different conditions [(a, b) Annealing treatment at 1400°C /30 min in microwave field and (c, d) Annealing treatment at 1450°C /6h in an electric oven. Scale : (a) and (c) - 2μm; (b) - 200 nm; (d) - 1μm ] / Imagini SEM ale probelor LSGM sinterizate la diferite temperaturi folosind mijloace diferite de încălzire. [(a, b) Tratament termic 1400°C /30 min în câmp de microunde , și (c,d) tratament termic 1450°C /6h în cuptor electric.

The average thermal expansion coefficient (TEC) of Sr- and Mg-doped LaGaO<sub>3</sub> has been investigated by various researchers [26-29]. Matching TEC of all the components of a SOFC is an important requirement for smooth running and long-term stability of such a system. On the other hand, repeated cycles of heating-cooling can drastically affects the assemble anode/electrolyte/cathode limiting the operating life of the device. TEC of LSGM electrolyte was measured for a cycle (heating-cooling) up to a temperature of 1000°C and the result is given in Fig. 8. The change of the specimen length would not be found after the thermal cycle if the volume change is isotropic. But the permanent strain appearing in dilatometric curve has non-isotropic characteristics. Previous studies have reported that transformation plasticity was responsible for the dimensional change undergoing thermal cycling [30]. The Fig. 8 and 9 indicate that as the temperature increases, TEC values also increases. TEC , for the temperature domain 400°C-800°C, of microwave sintered samples was  $9.22 \times 10^{-6}/^{\circ}\text{C}$ . For the same domain the samples sintered in electric furnace show TEC value of  $9.81 \times 10^{-6}/^{\circ}\text{C}$ . The values of TEC are in accordance with literature data [31] or lower [26]. This difference is attributed to the presence of the secondary phase and morphology of the material. Comparing with a most communally used anode (Ni-YSZ -  $\alpha_{(300-1000)} = 12.5 \times 10^{-6}/^{\circ}\text{C}$ ) or (LaSr)MnO<sub>3-x</sub> cathodes the

present work are lower but may fit in the intermediate operating temperatures domain.

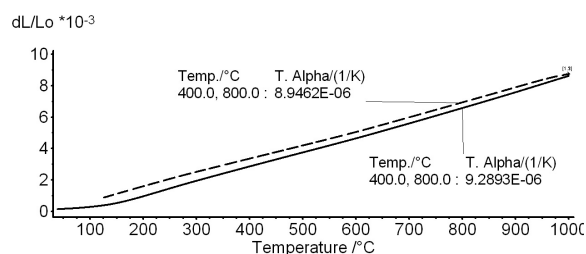


Fig. 8 - Dilatometric curves of microwave activated LSGM samples (1400°C/30min) showing length change of specimen after a thermal cycle (dash line- cooling) / Curbele dilatometrice ale probelor tratate în câmp de microunde (1400°C/30 min) demonstrând modificările ca urmare a unui ciclu termic încălzire-răcire (linia punctată - racier).

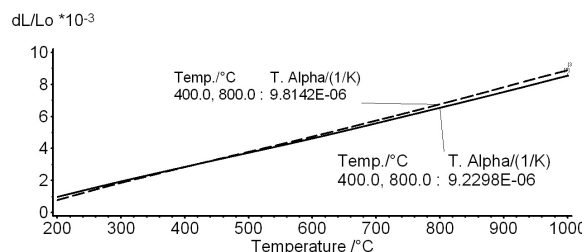


Fig. 9 - Dilatometric curves of microwave activated LSGM (1400°C/30min) samples and electrically heated sample (1450°C/6h -dashed line) / Curbele dilatometrice ale probelor obținute în câmp de microunde (1400°C/30min) și în cuptor electric (1450°C/6h -linie punctată)

values obtained for LSMG electrolytes in the Fig. 9 the thermal expansion curve of the LSGM sample sintered in microwave field is presented in comparison with the similar curve obtained for the samples sintered by conventional sintering in electric oven. It is important to note that the two curves intersect at around 450°C, TEC values becoming greater in the case of LSGM bodies annealed in the electric oven. That can be explained by the different morphologies of the two materials, in accordance with SEM observation.

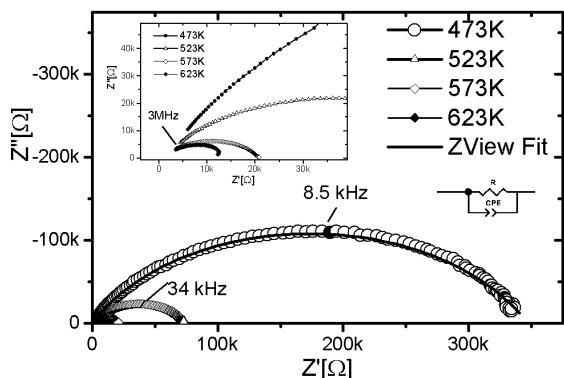


Fig. 10 - Nyquist plot of impedance spectra measured on microwave sintered sample at different temperatures. Inset: The impedance spectra at high frequencies and the equivalent electrical circuit used for fitting data / *Reprezentarea grafică Nyquist a spectrelor de impedanță măsurate pe probele sinterizate în câmp de microunde la diferite temperaturi. Insetat: Spectrele de impedanță la frecvență ridicată și circuitul echivalent folosit la ajustarea datelor.*

On the sintered samples their electrical properties were also determined. In the Fig. 10 the imaginary part of the impedance is plotted versus real part of the impedance for several temperatures. There is only one semicircle which suggests that the bulk and grain boundary processes are strongly overlapping. Consequently, is not possible to resolve the bulk and grain boundary conductivities. Only the total conductivity of the sample can determine by fitting the semicircle with the response of an (R CPE (constant phase element)) parallel circuit [32]. The electrical conductivities of the samples were calculated from impedance data using the formula:

$$\sigma = \frac{t}{A \times R}$$

where  $t$  and  $A$  represent the thickness and area of the sample surface.

The total conductivities of the microwave sintered sample and of the classical sintered sample were compared in an Arrhenius plot in Figure 11. The electrical conductivities of our samples were around those reported in the literature [3,5] but the conductivities of microwave sintered sample were increased after the MW treatment over entire temperature range. This result is demonstrating that the MW treatment is improving the electrical proprieties of sample. For example at 700 °C the electrical conductivity is

48% higher – 14.4 mS/cm of MW sample compared with 9.7 mS/cm of classically annealed sample.

This variation of the conductivity can be attributed to differences in the microstructure of the samples.

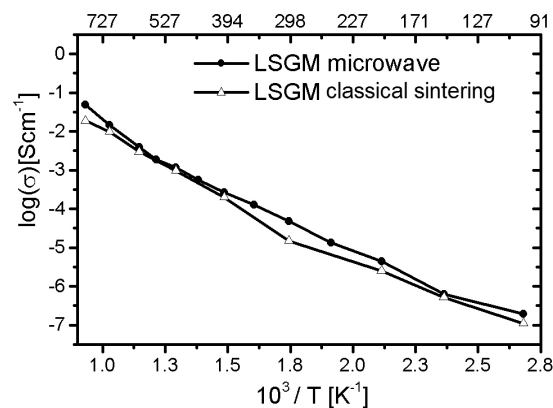


Fig. 11 - Arrhenius plot of the total conductivities measured on microwave sintered samples and on conventionally sintered samples / *Reprezentarea Arrhenius a măsurătorilor de conductivitate electrică totală efectuate pe probele sinterizate în câmp de microunde și convențional (cuptor electric).*

#### 4. Conclusion

Doped lanthanum gallate ( $\text{La}_{0.8}\text{Sr}_{0.2}\text{Ga}_{0.83}\text{Mg}_{0.17}\text{O}_{2.815}$ ) can be prepared as almost a single perovskite phase by a modified Pechini method using polyvinyl alcohol (PVA) as polyhydric alcohol. Fine, homogeneous and high density pellets of almost pure LSGM phase were obtained after sintering at 1400°C for a short period time in an activated microwave field.

The XRD pattern shows that the perovskite phase (LSGM) exists in the unsintered powders resulted after calcination in an electric oven at 900°C for 1 hour. Annealing at temperatures higher than 1000°C promotes the obtaining of dimensional homogeneity of the submicron grains. For the same composition, the sintering method may influence the symmetry of the perovskite phase (LSGM): orthorhombic, when microwave irradiation was used and cubic in the case of conventional heating. According to our experiments a supplementary annealing of the resin at around 900°C enhanced the quantity of the LSGM phase. Due to the heat generation *in situ* by microwave irradiation, the process of sintering is activated with faster kinetics compared to a conventional sintering technique and thereby, denser ceramics, free of intergranular porosity can be obtained.

#### Acknowledgements

We thank to the financial support of the POS CCE project INFRANANOCHEM/2011 and PNII/2010 MATSOFC 71030



REFERENCES

1. T. Ishihara, H. Matsuda, Y. Takita, Doped LaGaO<sub>3</sub> perovskite type oxide as a new oxide ionic conductor, J. Am. Chem.Soc., 1994, **116**, 3801.
2. M. Feng, J. B. Goodenough, A superior oxide ion electrolyte, Eur. J. Solid State Inorg. Chem., 1994, **31**, 663
3. P.N. Huang, A. , Superior oxygen ion conductivity of lanthanum gallate doped with strontium and magnesium, J. Electrochem. Soc., 1996, **143**, 644.
4. M. Feng, J.B.Goodenough, K.Huang, C.Mulliken, Fuel cells with doped lanthanum gallate electrolyte, J. Power Sources 1996, **63**, 47.
5. K. Huang, R.S Tichy, J.B. Goodenough, Superior perovskite oxide-ion conductor Strontium- and magnesium-doped LaGaO<sub>3</sub>: I, phase relationships and electrical properties, J. Am. Ceram. Soc. 1998, **81**, 2565.
6. V. Fruth, C. Andronescu, C. Hornoiu, C.Tenea, A.Rusu, R. Scurtu, Processing of (La,Sr)(Ga,Mg)O<sub>3</sub> solid electrolyte using an enhanced solid state technique, Romanian Journal of Materials, 2011, **41**(1), 56.
7. S. Li, B. Bergman, Doping effect on secondary phases, microstructure and electrical conductivities of LaGaO<sub>3</sub> based perovskites, J Eur. Ceram., Soc. 2009, **29**, 1139.
8. M. Shi, N. Liu, Y. Xu, Y. Yuan, P. Majewski, F. Aldinger, Synthesis and characterization of Sr- and Mg-doped LaGaO<sub>3</sub> by using glycine–nitrate combustion method, J. Alloys Compd., 2006, **425**, 348.
9. K.Q. Huang, J.B. Goodenough, Wet Chemical Synthesis of Sr- and Mg-Doped LaGaO<sub>3</sub>, a Perovskite-Type Oxide-Ion Conductor, J. Solid State Chem. 1998, **136**, 274.
10. K.Q. Huang, M. Feng, J.B. Goodenough, Sol-Gel Synthesis of a New Oxide-Ion Conductor Sr- and Mg-Doped LaGaO<sub>3</sub> Perovskite, J. Am. Ceram. Soc., 1996, **79**, 1100.
11. J.G. Li, T. Ikegami, T. Mori, T. Wada, Reactive Ce<sub>0.8</sub>Re<sub>0.2</sub>O<sub>1.9</sub> (RE = La, Nd, Sm, Gd, Dy, Y, Ho, Er, and Yb) powders via carbonate coprecipitation, Sintering Chem. Mater., 2001, **13**, 2921.
12. I. Stijepovic, A. J. Darbandi, V. V. Sradic, Conductivity of doped LaGaO<sub>3</sub> prepared by citrate sol-gel method, J. Optoelect. And Adv. Mater., 2010, **12**, 1098.
13. J.W. Stevenson, T.R. Armstrong, L.R. Pederson, J. Li, C.A. Lewinsohn, S. Baskaran, Effect of A-site cation nonstoichiometry on the properties of doped lanthanum gallate, Solid State Ionics 1998, **115**, 571.
14. M.P. Pechini, US Patent No.3.330.697 July 1(1967).
15. B. Rambabu, S. Ghosh, W. Zhao, and H. Jena, Innovative processing of dense LSGM electrolytes for IT-SOFC's, J. Power Sources 2006, **159**, 21.
16. S. Boldrini, C.Mortalò, S.Fasolin, F. Agresti, L.Doubova, M.Fabrizio and S.Barison , Influence of Microwave-Assisted Pechini Method on La<sub>0.80</sub>Sr<sub>0.20</sub>Ga<sub>0.83</sub>Mg<sub>0.17</sub>O<sub>3-d</sub> Ionic Conductivity, Fuel Cells 2012, **12**, 54.
17. D. S. Junga, H. Y. Kooa, H. C. Janga, J. H. Kima, Y. H. Chob, J.H. Leeb, Y. C. Kanga, Firing characteristics of La<sub>0.8</sub>Sr<sub>0.2</sub>Ga<sub>0.8</sub>Mg<sub>0.2</sub>O<sub>3</sub>-electrolyte powders prepared by spray pyrolysis, J. Alloys Compd., 2009, **487**, 693.
18. T. Mathews, R. Subasri, O.M.Sreedharan, A rapid combustion synthesis of MgO stabilized Sr- and Ba-β-alumina and their microwave sintering , Solid State Ionics 2002, **243**, 135.
19. R. Harpeness, A. Gedanken, A. M. Weiss, and M. A. Slifkin, Microwave-assisted synthesis of nanosized MoSe<sub>2</sub>, J. Mater. Chem. 2003, **13**, 2603.
20. N. Masanobu, K. Watanabe, I. Hiromasa, U. Yoshiharu, W. Masataka, Grain size control of LiMn<sub>2</sub>O<sub>4</sub> cathode material using microwave synthesis method, Solid State Ionics 2003, **164**, 35.
21. V. Subramanian, C. L.Chen, H. S. Chou, and T. K. Fey, Microwave-assisted solid-state synthesis of LiCoO<sub>2</sub> and its electrochemical properties as a cathode material for lithium batteries, J. Mater.Chem. 2001, **11**, 3348.
22. R. Subasri, T. Mathews, and O.M. Sreedharan, Microwave assisted synthesis and sintering of La<sub>0.8</sub>Sr<sub>0.2</sub>Ga<sub>0.83</sub>Mg<sub>0.17</sub>O<sub>2.815</sub> , Mater. Lett. 2003, **57**, 1792.
23. C. Gabriel, S. Gabriel, E. H. Grant, B. S. J. Halstead, and D. M. P. Mingos, Dielectric parameters relevant to microwave dielectric heating, Chem. Soc. Rev. 1998, **27**, 213.
24. A.C. Tas, P.J. Majewski and F. Aldinger, Chemical Preparation of Pure and Strontium and/or Magnesium-doped Lanthanum Gallate Powders, J.Am. Ceram. Soc. 2000, **83**, 2954.
25. P. R. Slater, J. T. S. Irvine, T. Ishihara, and Y. Takita, The Structure of the Oxide Ion Conductor La<sub>0.9</sub>Sr<sub>0.1</sub>Ga<sub>0.8</sub>Mg<sub>0.2</sub>O<sub>2.85</sub> by Powder Neutron Diffraction, Solid State Ionics, 1998, **107**, 319.
26. P. Datta, P. Majewski, and F. Aldinger, Thermal expansion behaviour of Sr- and Mg-doped LaGaO<sub>3</sub> solid electrolyte, J. Eur. Ceram. Soc., 2009, **29**, 1463.
27. M. Rozumek, P. Majewski, L. Sauter, and F. Aldinger, La<sub>1-x</sub>Sr<sub>1-x</sub>Ga<sub>3</sub>O<sub>7-δ</sub> melilite-type ceramics: preparation, composition and structure, J. Am. Ceram. Soc., 2004, **87**, 662.
28. A. L. Shaula, V. V. Kharton, F. M. B. Marques, A. V. Kovalevsky, A. P. Viskup, and E. N. Naumovich, Oxygen permeability of mixed-conducting composite membranes: effects of phase interaction, J. Solid State Electrochem., 2006, **10**, 28.
29. V.V. Kharton, F.M.B. Marques, and A. Atkinson, Transport properties of solid oxide electrolyte ceramics: a brief review, Solid State Ionics 2004, **174**, 135.
30. D.W. Suh, C.S. Oh, H.N. Han, and S.J. Kim, Dilatometric analysis of austenite decomposition considering the effect of non-isotropic volume change, Acta Materialia, 2007, **55**(8), 2659.
31. F.Tietz, Thermal Expansion of SOFC Materials, Ionics 1999, **5**, 129.
32. P. Mondal, A. Klein, W. Jaegermann, and H. Hahn, Enhanced specific grain boundary conductivity in nanocrystalline Y<sub>2</sub>O<sub>3</sub>-stabilized zirconia, Solid State Ionics 1999, **118**, 331.

\*\*\*\*\*